MNRAS **000**, 1–24 (2015) Preprint 5 June 2019 Compiled using MNRAS LATEX style file v3.0

Appendix: 11 γ Dor stars with rotational splittings

Gang Li[1,3★], Timothy Van Reeth[1,2,3], Timothy R. Bedding[1,3†], Simon J. Murphy[1,3], Victoria Antoci[3], Rhita-Maria Ouazzani[4], Nicholas H. Barbara[1,3]

[1] *Sydney Institute for Astronomy (SIfA), School of Physics, 2006 University of Sydney, Australia*
[2] *Institute of Astronomy, KU Leuven, Celestijnenlaan 200D, B-3001 Leuven, Belgium*
[3] *Stellar Astrophysics Centre, Department of Physics and Astronomy, Aarhus University, Ny Munkegade 120, DK-8000 Aarhus C, Denmark*
[4] *LESIA, Observatoire de Paris, PSL Research University, CNRS, Sorbonne Universités, UPMC Univ. Paris 06, Univ. Paris Diderot, Sorbonne Paris Cité, 5 place Jules Janssen, 92195 Meudon, France*

Accepted XXX. Received YYY; in original form ZZZ

ABSTRACT

We present the period spacing patterns, the splitting identifications, the splitting variations, and the TAR fittings of 11 γ Dor stars. These stars are interesting because rotational splittings are rare among rapid rotators. The inclinations of these stars should be very small so the tesseral modes are seen, based on the amplitude distribution theory.

Key words: stars: oscillations – stars: rotation – stars: variables

★ E-mail: gali8292@uni.sydney.edu.au
† E-mail: tim.bedding@sydney.edu.au

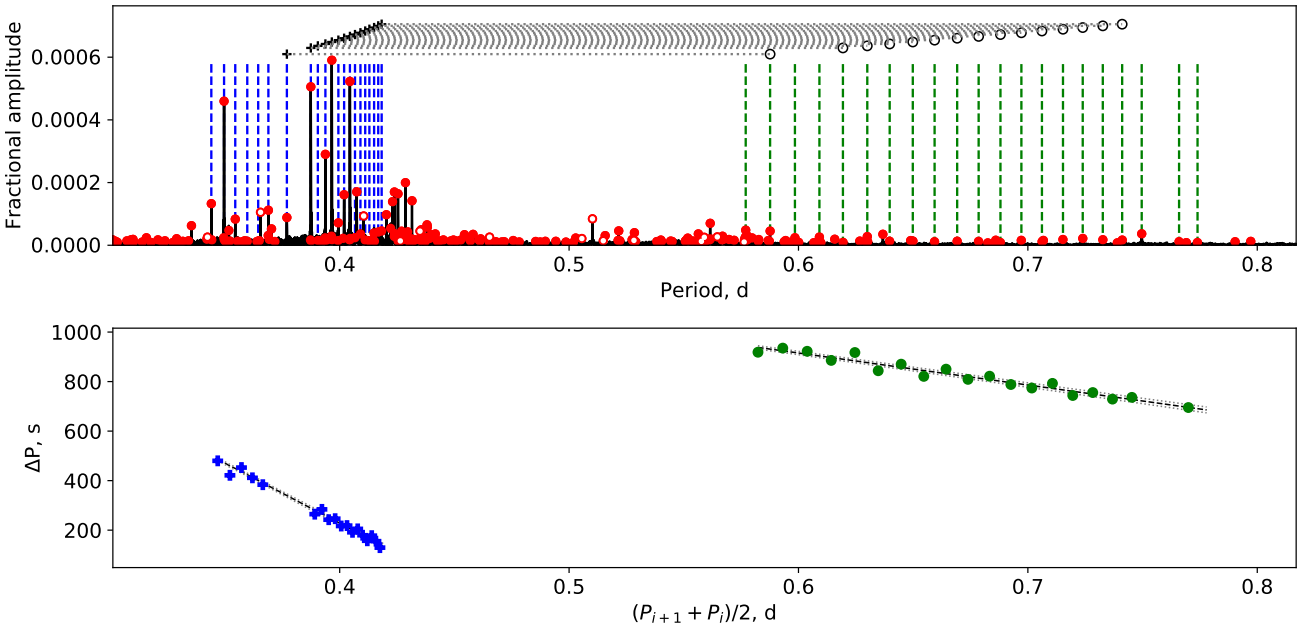

Figure 1. The amplitude spectrum and period-spacing patterns of KIC 5476473. Top panel: the amplitude spectrum as a function of period. The red dots are the extracted frequencies and the open dots show the likely combination frequencies. The vertical dashed lines show the observed periods. Two period-spacing patterns are seen. The blue dashed lines (left) are the $l = 1, m = 1$ g modes. The green dashed lines (right) are the $l = 1, m = 0$ g modes. Above the spectrum '+' is the $m = 1$ mode and 'O' is the $m = 0$ mode. The horizontal dotted lines connect the modes with same radial order n. Bottem: the peirod spacing patterns. The left one is the $l = 1, m = 1$ g modes while the right one is $l = 1, m = 0$ g modes. The linear fits and uncertainties are shown by the black and gray dashed lines, with dips removed.

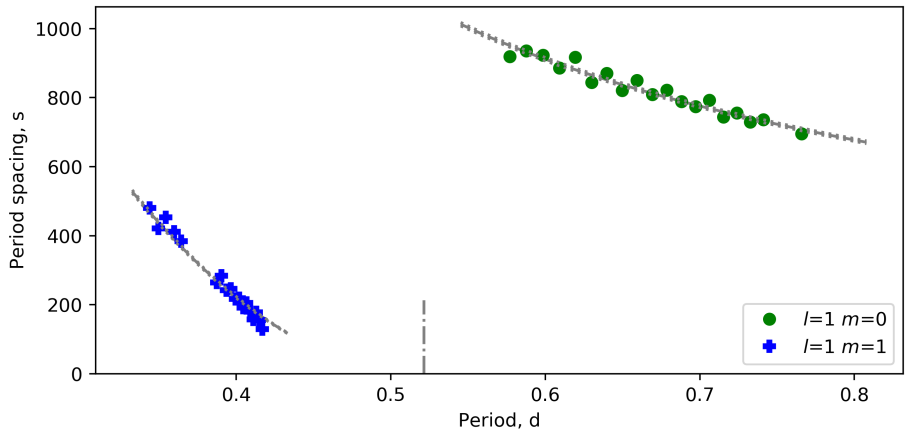

Figure 2. The best fitting period spacings of KIC 5476473.

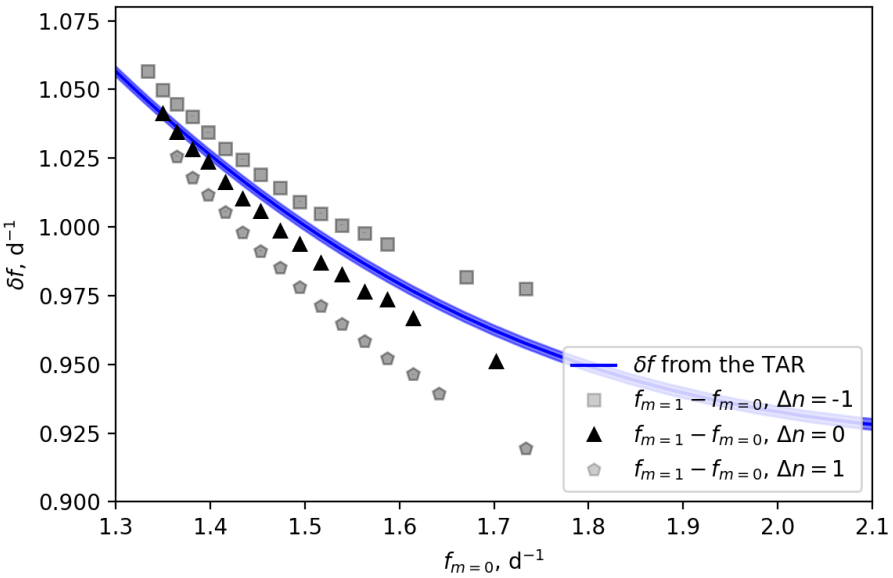

Figure 3. The splitting variation as a function of frequency of KIC 5476473. The blue line and shaded area are the predicted curve and uncertainty from the TAR fitting result. The black squares are the splittings which follow the theory best. The grey symbols are the splittings whose radial orders are mismatched by a factor of ±1.

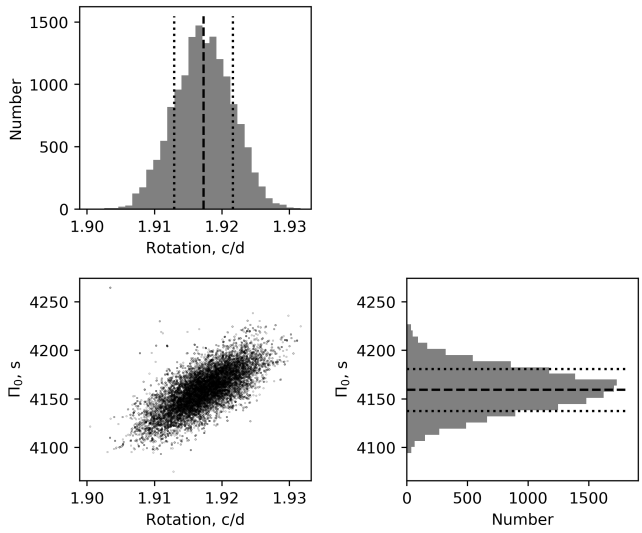

Figure 4. The 2D posterior distributions of KIC 5476473.

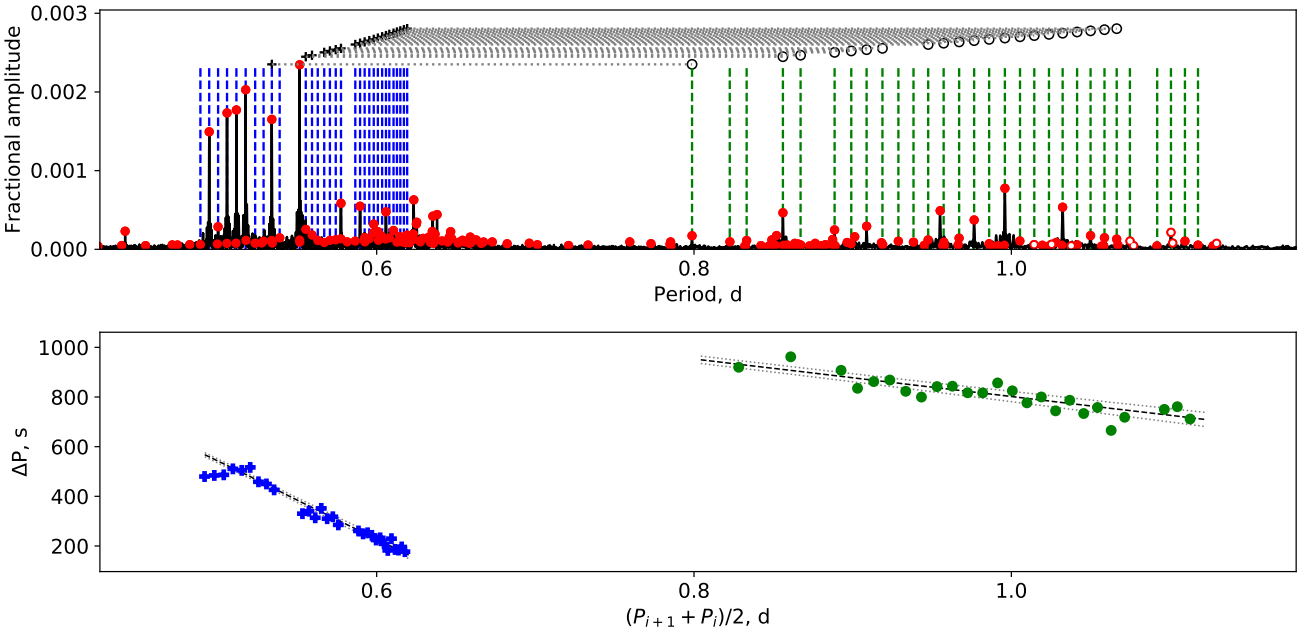

Figure 5. The period spacing patterns of KIC 4846809.

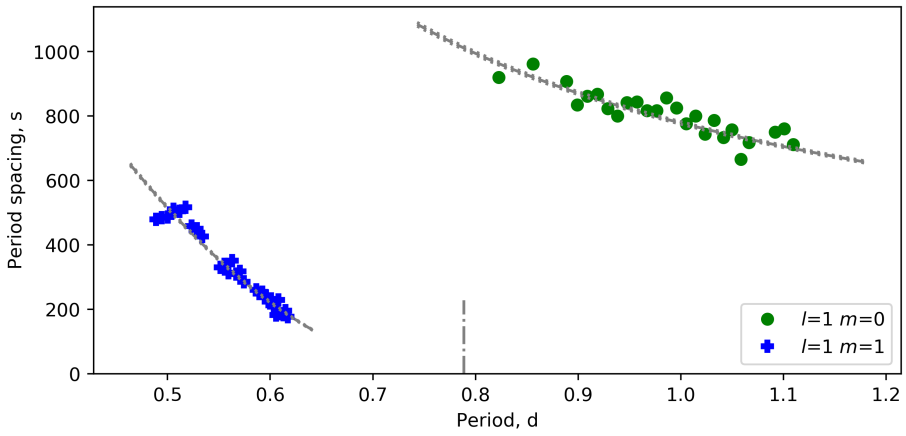

Figure 6. The best fitting period spacings of KIC 4846809.

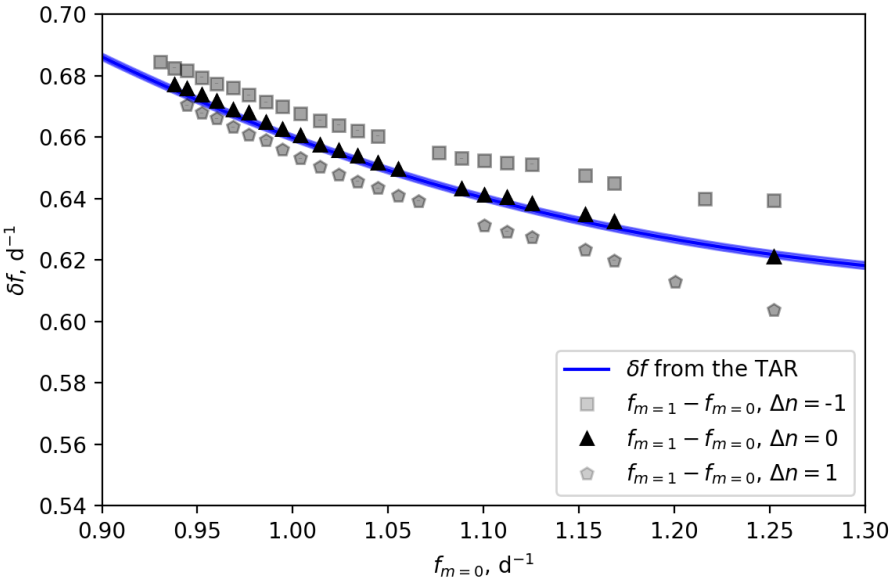

Figure 7. The observed and theoretical splittings of KIC 4846809.

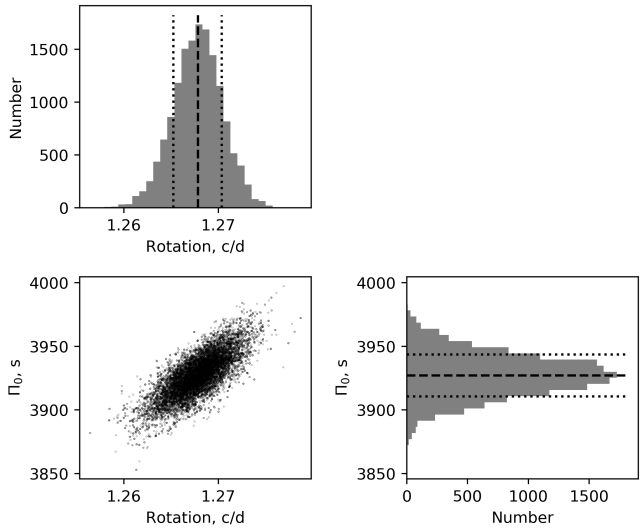

Figure 8. The 2D posterior distributions of KIC 4846809.

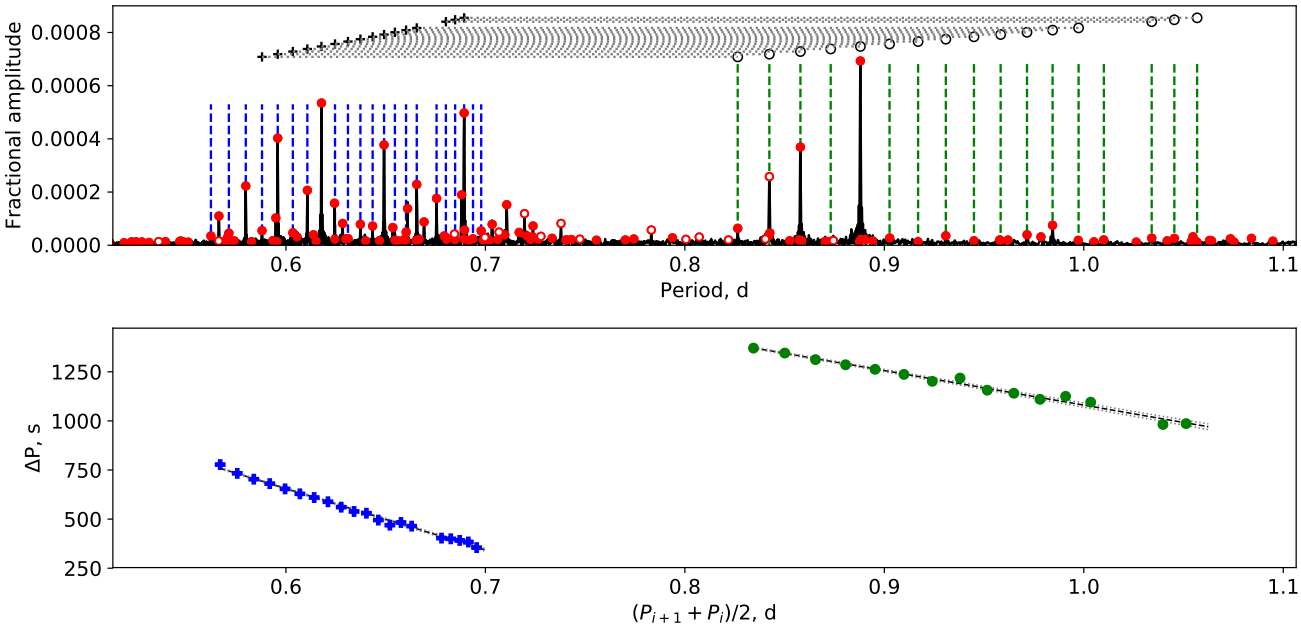

Figure 9. The period spacing patterns of KIC 7778114.

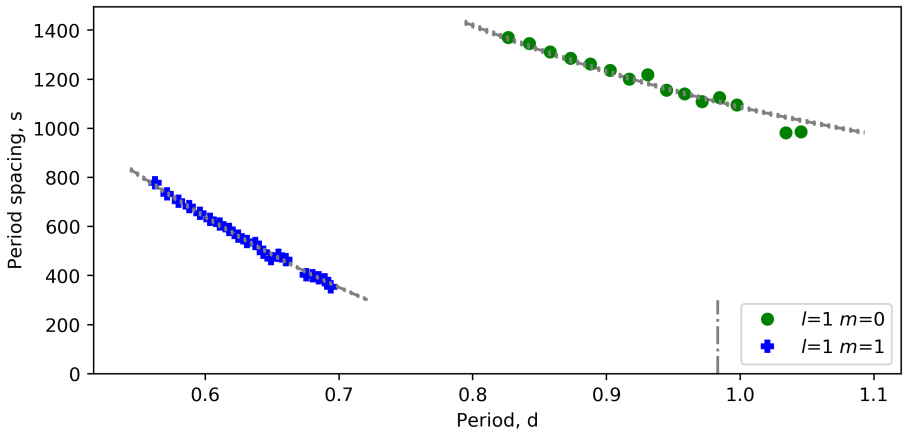

Figure 10. The best fitting period spacings of KIC 7778114.

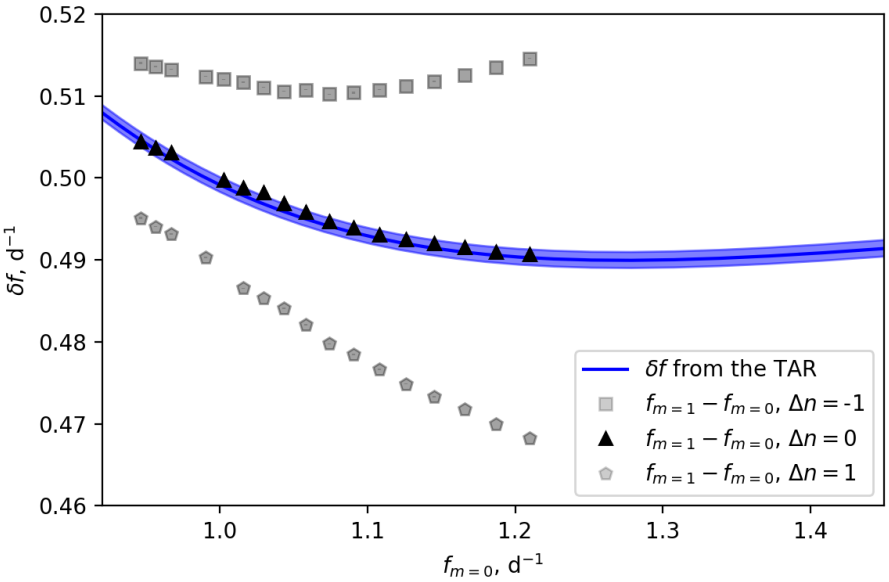

Figure 11. The observed and theoretical splittings of KIC 7778114.

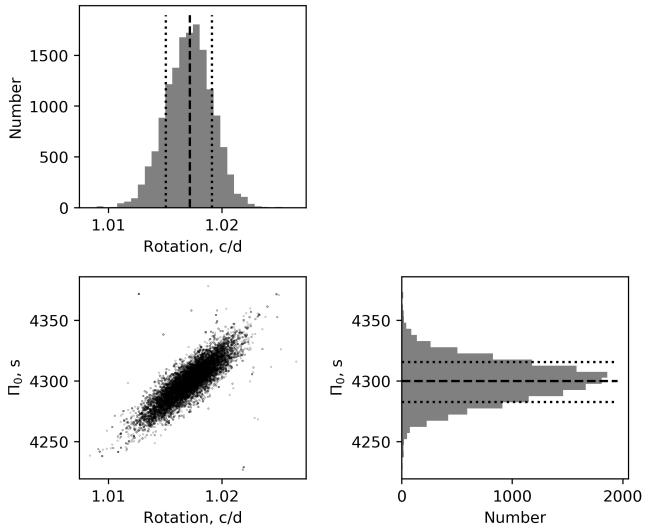

Figure 12. The 2D posterior distributions of KIC 7778114.

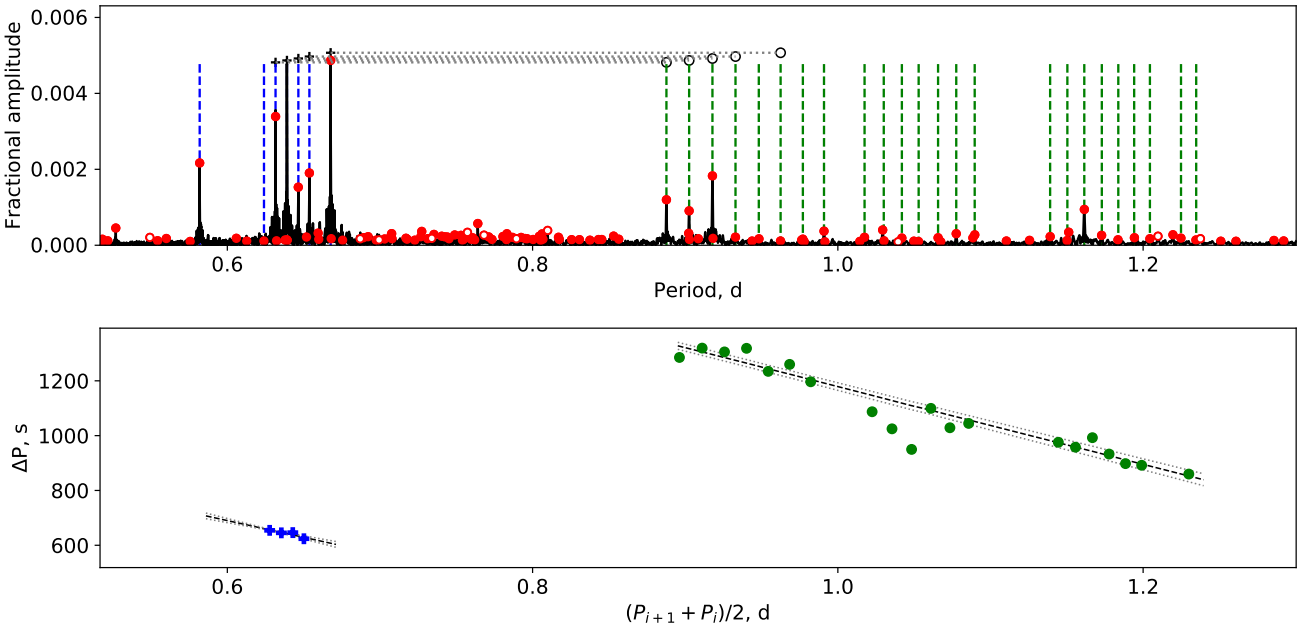

Figure 13. The period spacing patterns of KIC 4285040.

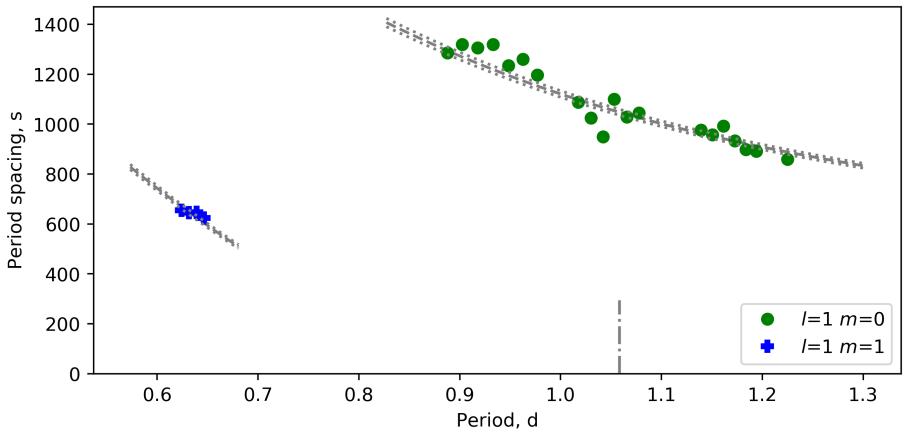

Figure 14. The best fitting period spacings of KIC 4285040.

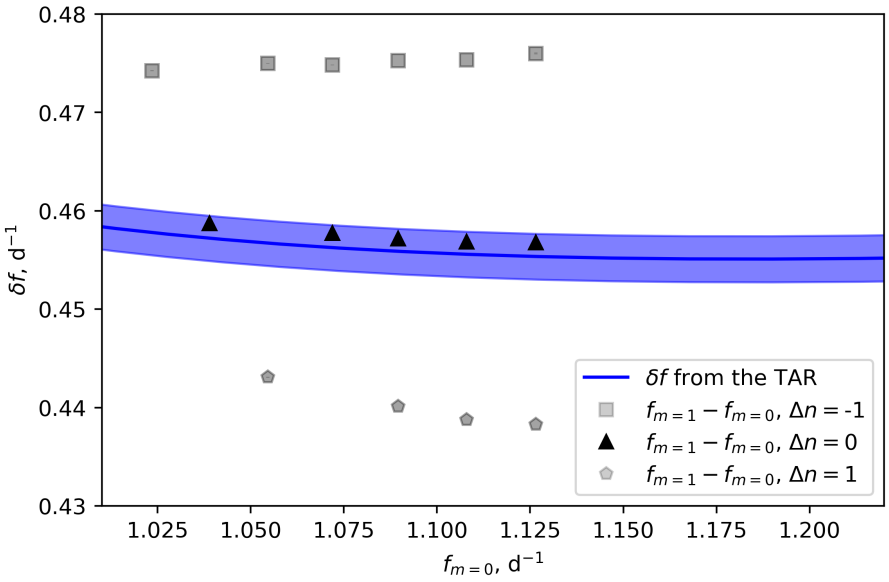

Figure 15. The observed and theoretical splittings of KIC 4285040.

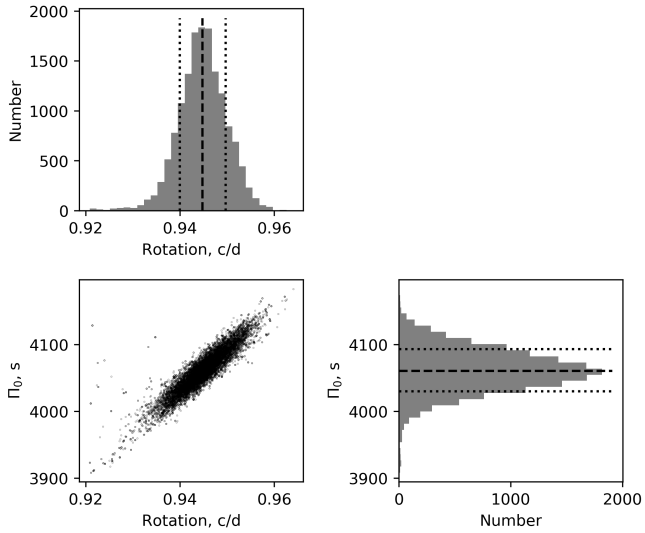

Figure 16. The 2D posterior distributions of KIC 4285040.

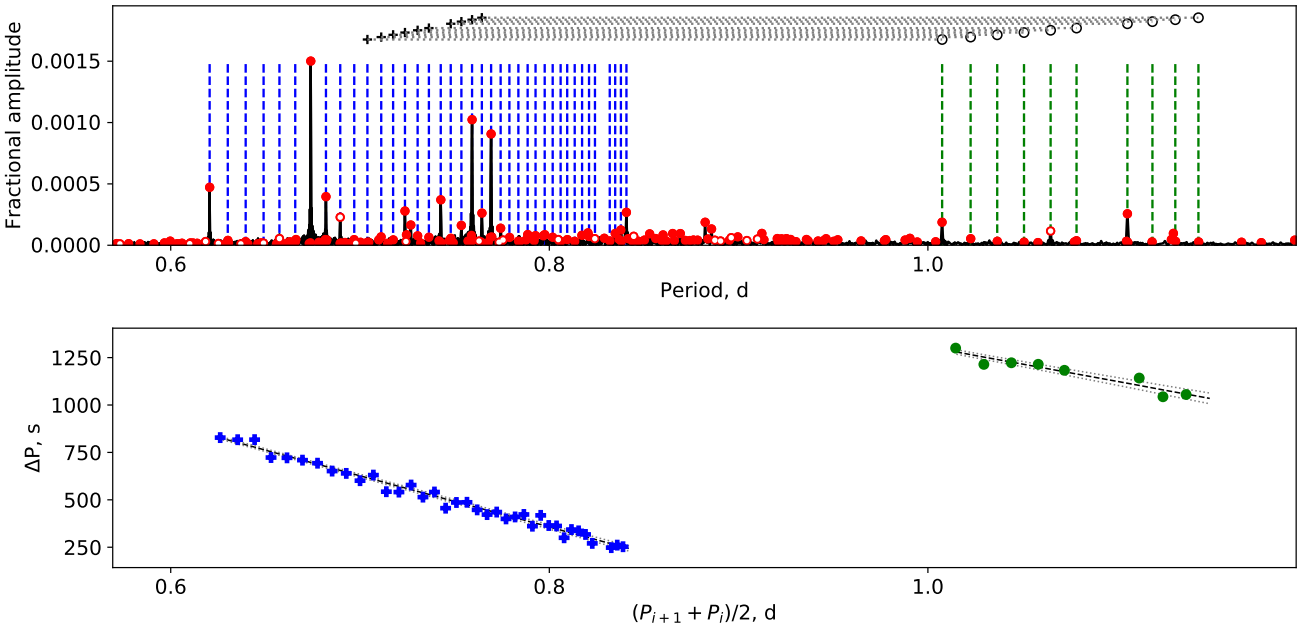

Figure 17. The period spacing patterns of KIC 12401800.

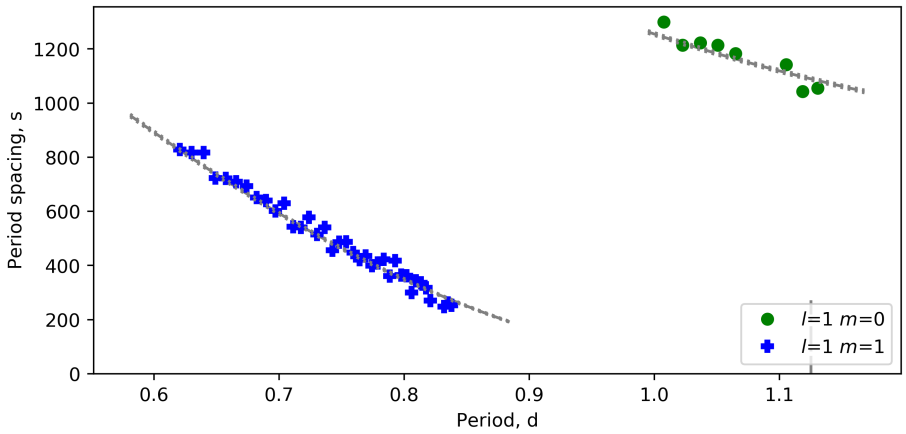

Figure 18. The best fitting period spacings of KIC 12401800.

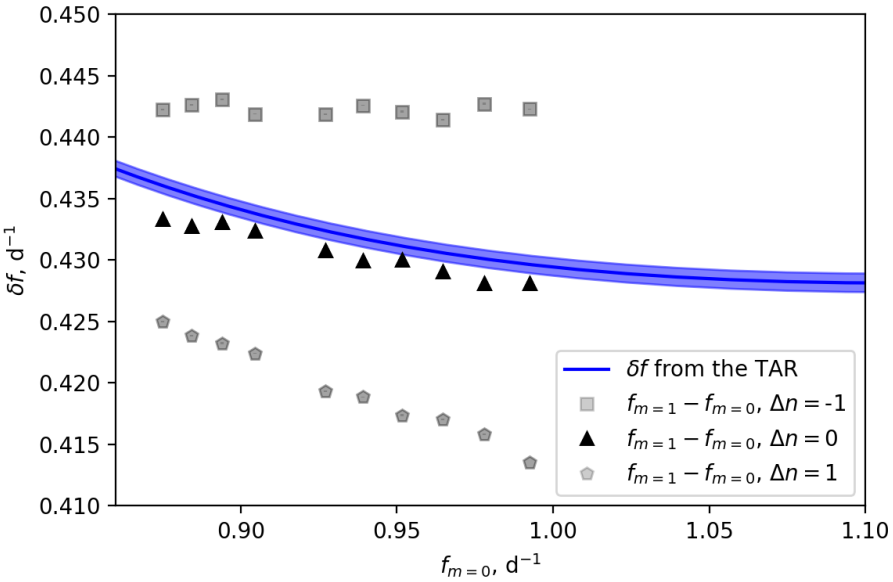

Figure 19. The observed and theoretical splittings of KIC 12401800.

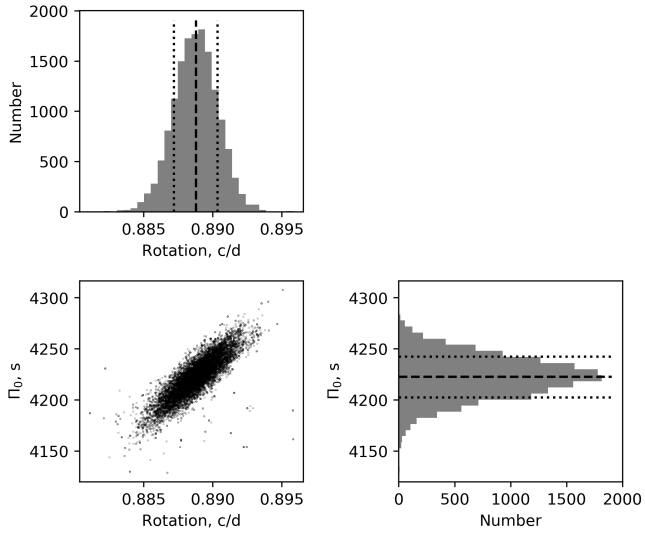

Figure 20. The 2D posterior distributions of KIC 12401800.

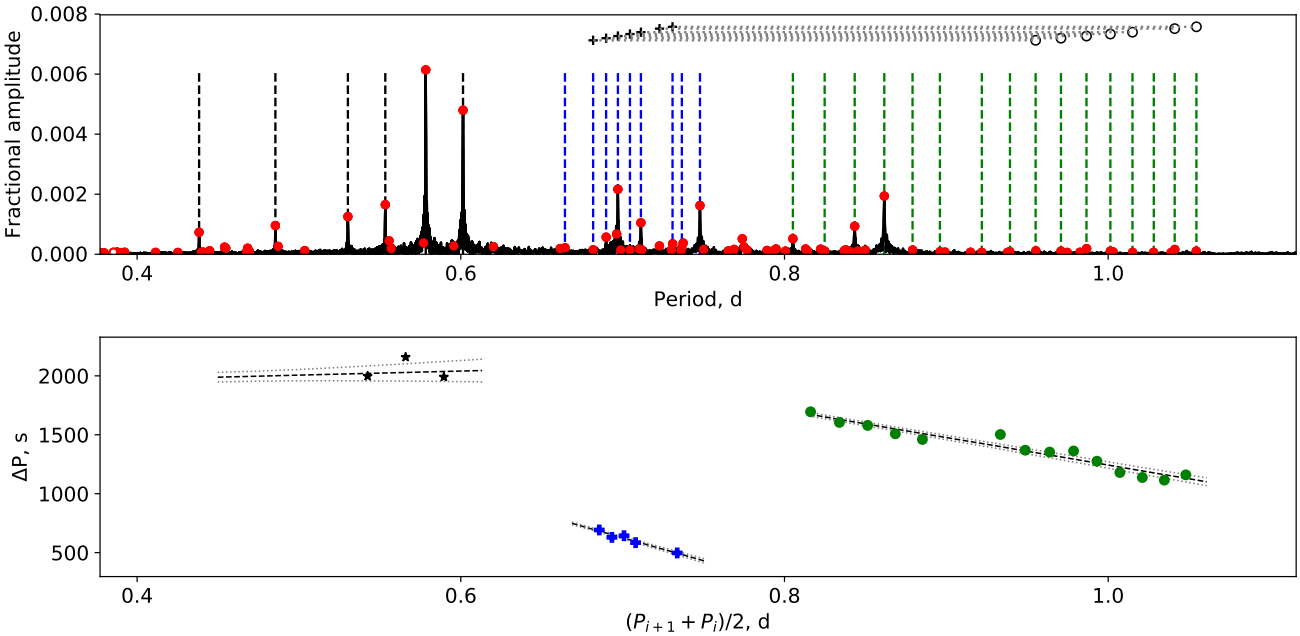

Figure 21. The period spacing patterns of KIC 9595743.

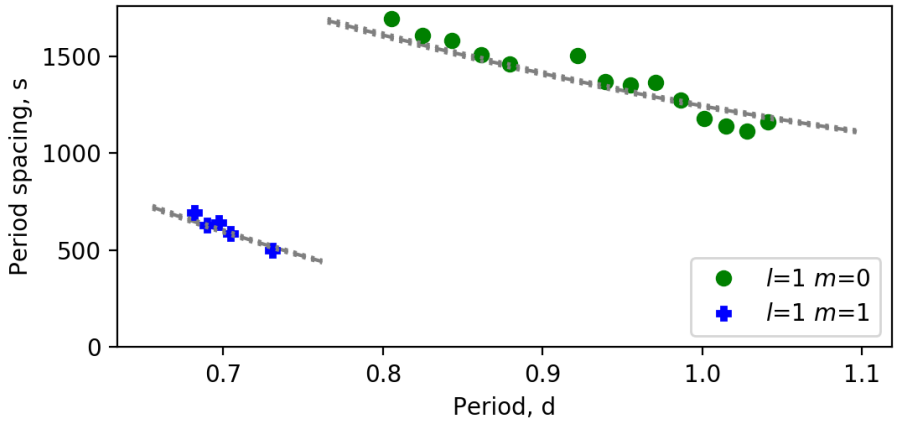

Figure 22. The best fitting period spacings of KIC 9595743.

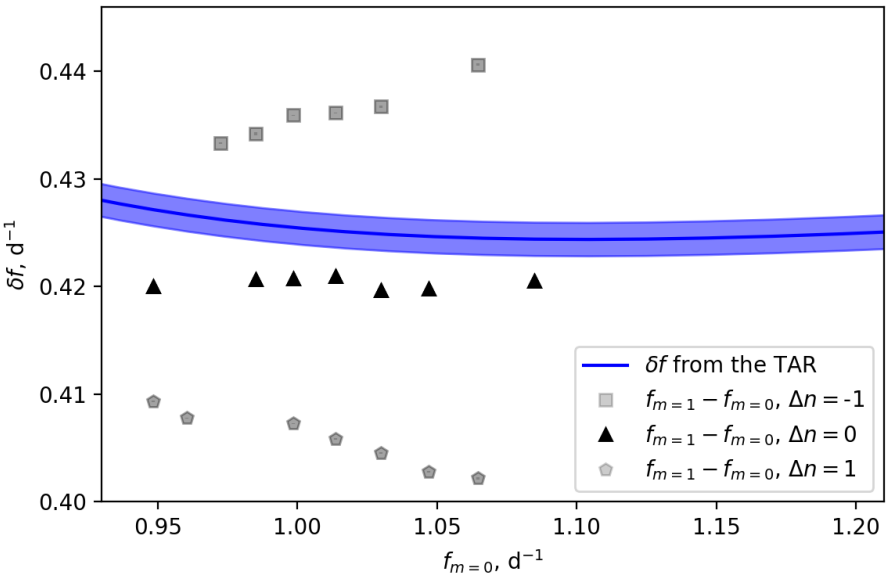

Figure 23. The observed and theoretical splittings of KIC 9595743.

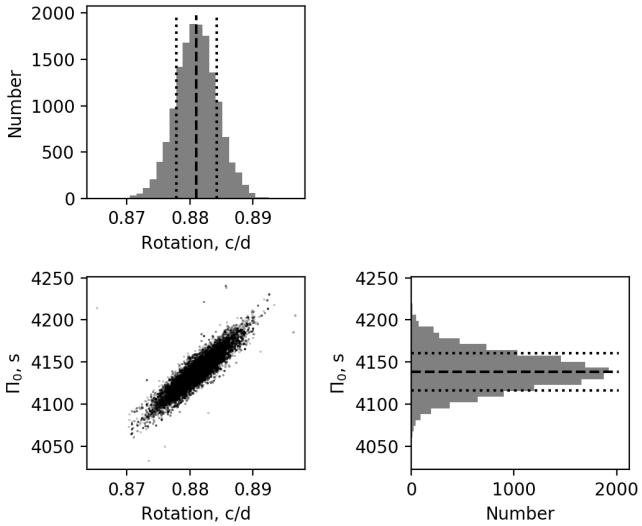

Figure 24. The 2D posterior distributions of KIC 9595743.

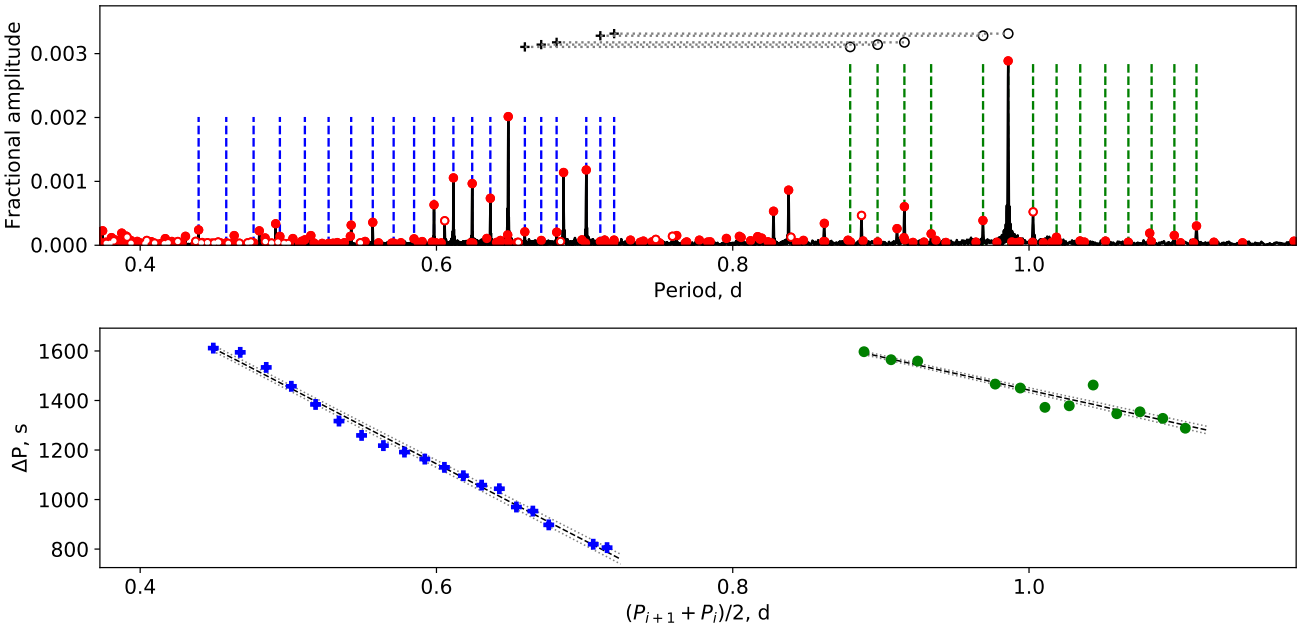

Figure 25. The period spacing patterns of KIC 3348714.

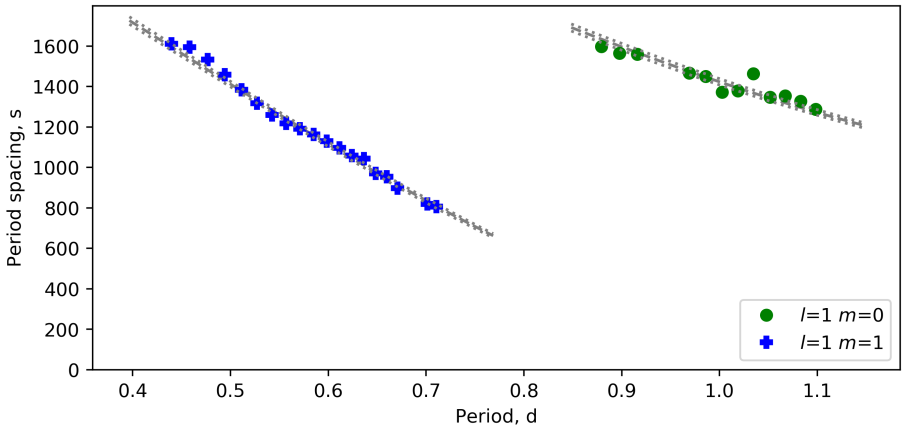

Figure 26. The best fitting period spacings of KIC 3348714.

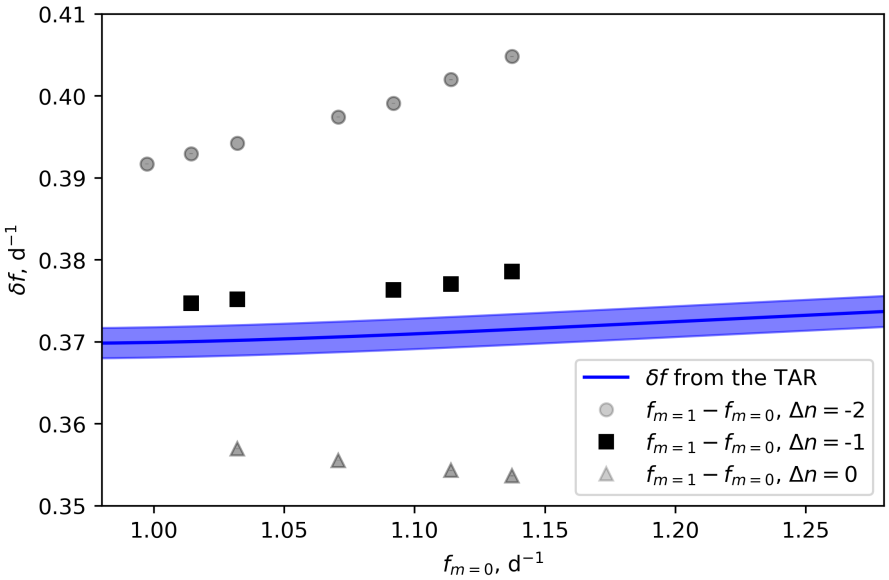

Figure 27. The observed and theoretical splittings of KIC 3348714.

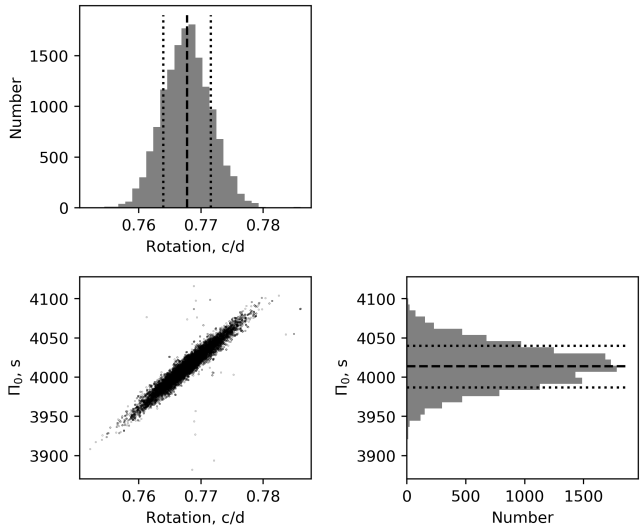

Figure 28. The 2D posterior distributions of KIC 3348714.

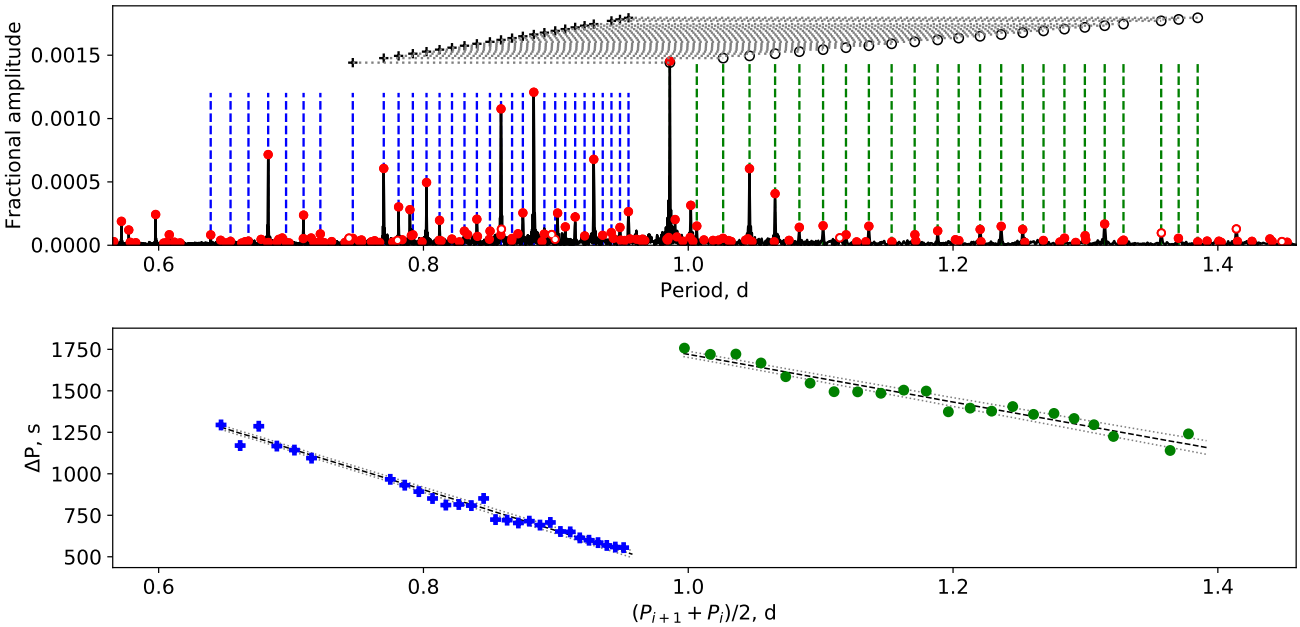

Figure 29. The period spacing patterns of KIC 7701947.

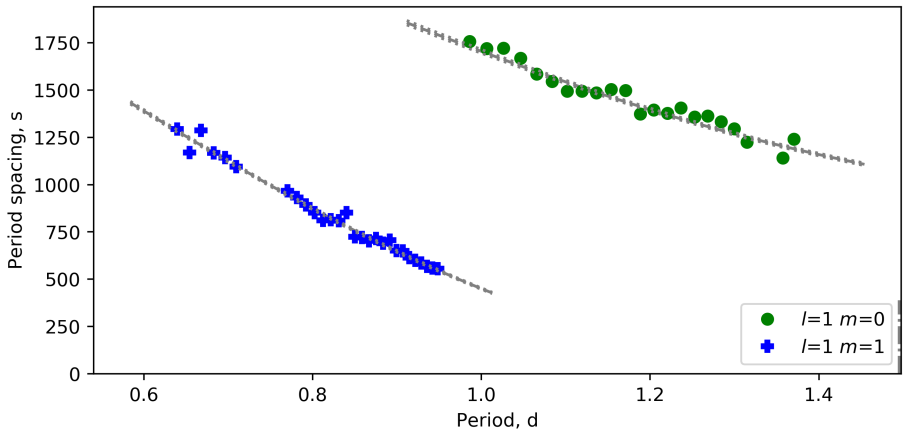

Figure 30. The best fitting period spacings of KIC 7701947.

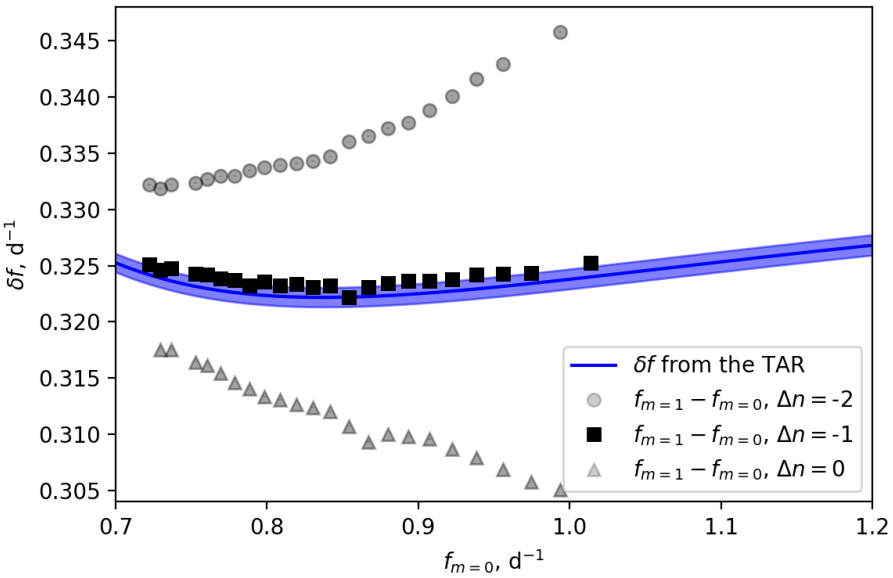

Figure 31. The observed and theoretical splittings of KIC 7701947.

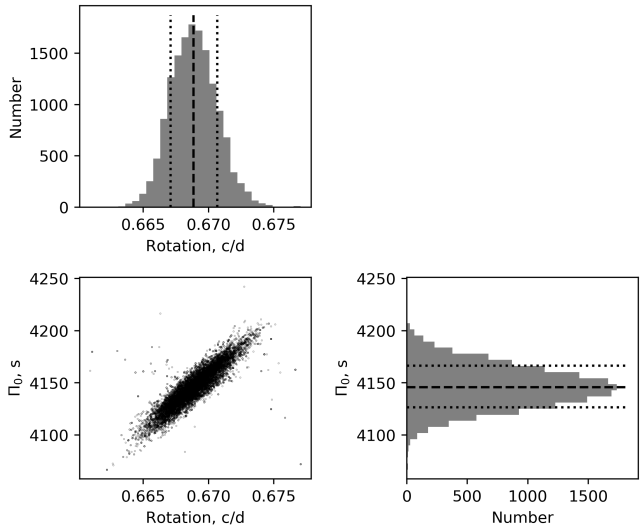

Figure 32. The 2D posterior distributions of KIC 7701947.

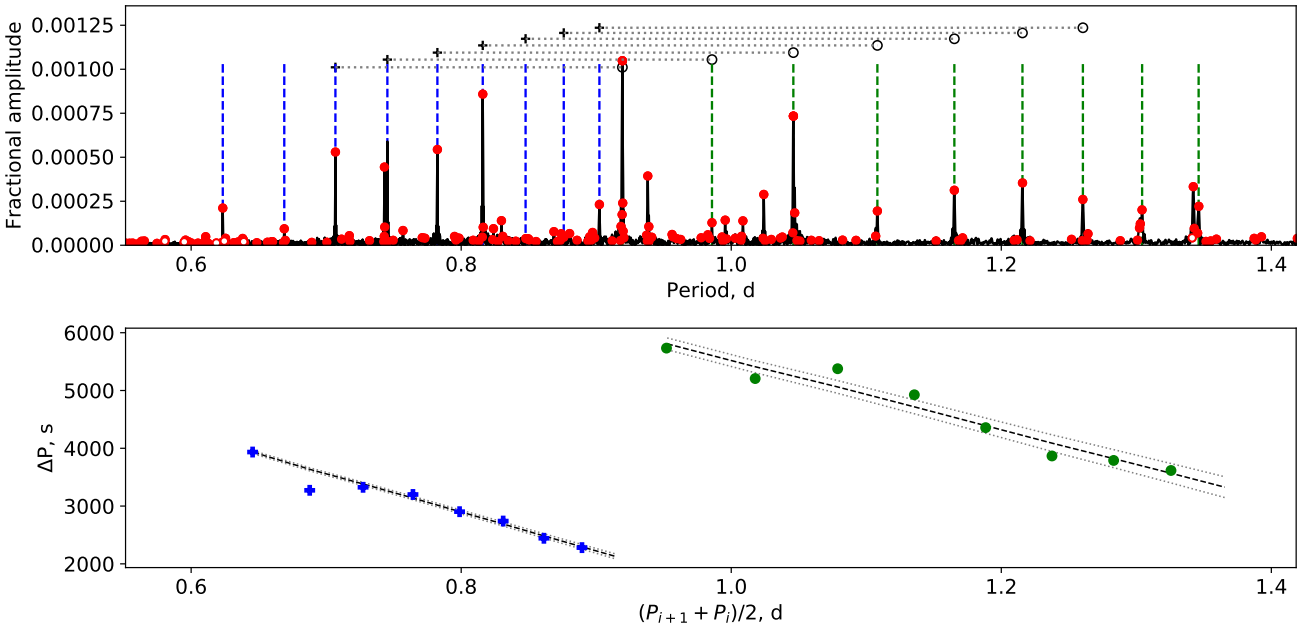

Figure 33. The period spacing patterns of KIC 8523871.

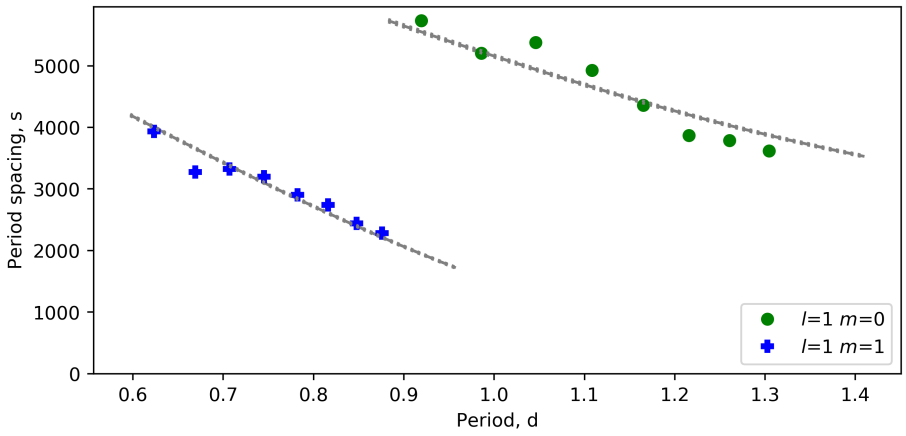

Figure 34. The best fitting period spacings of KIC 8523871.

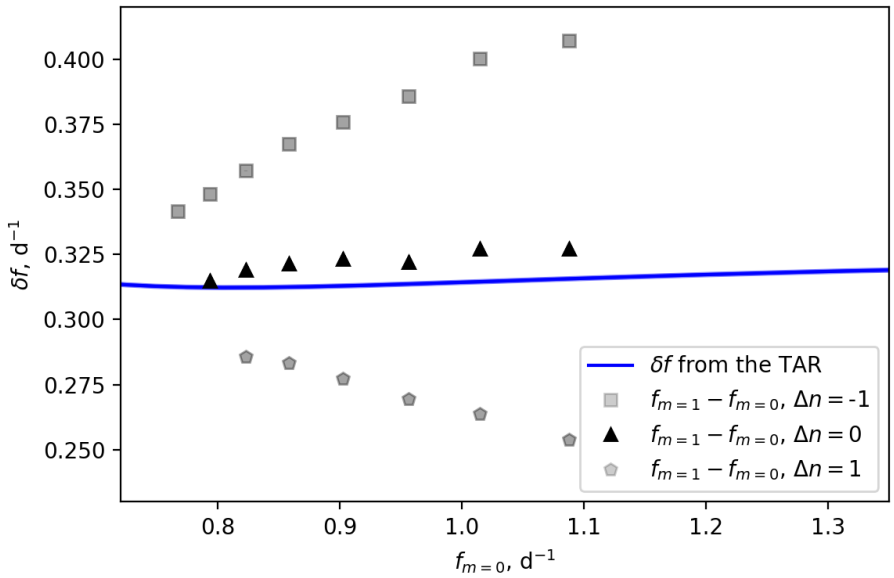

Figure 35. The observed and theoretical splittings of KIC 8523871.

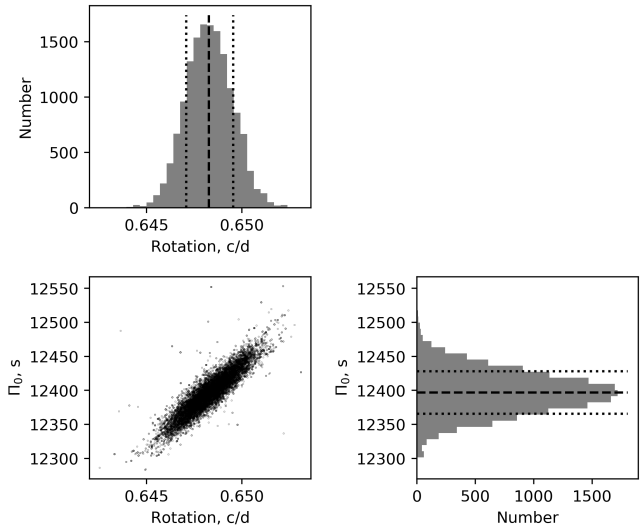

Figure 36. The 2D posterior distributions of KIC 8523871.

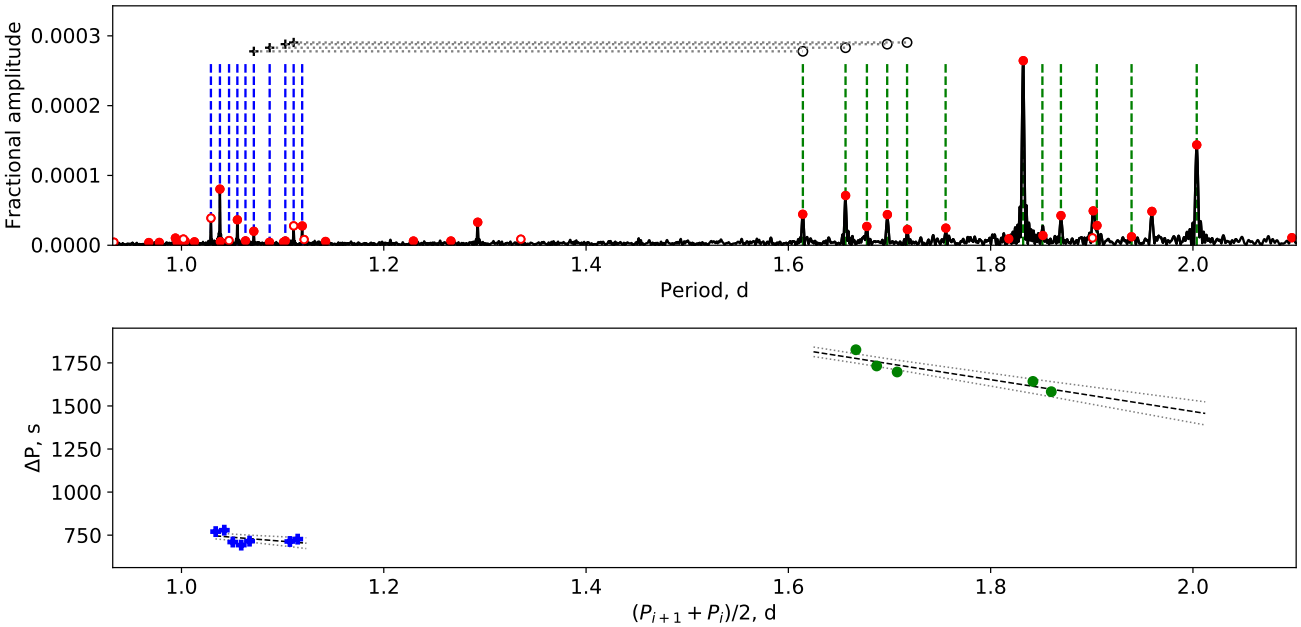

Figure 37. The period spacing patterns of KIC 4952246.

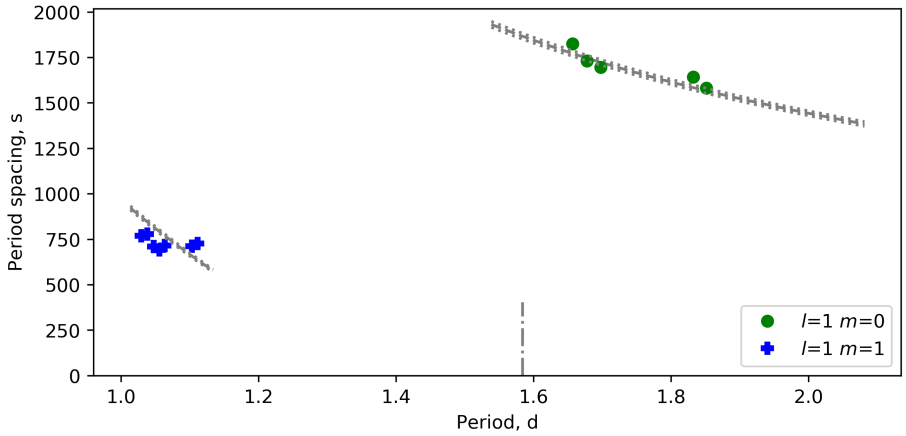

Figure 38. The best fitting period spacings of KIC 4952246.

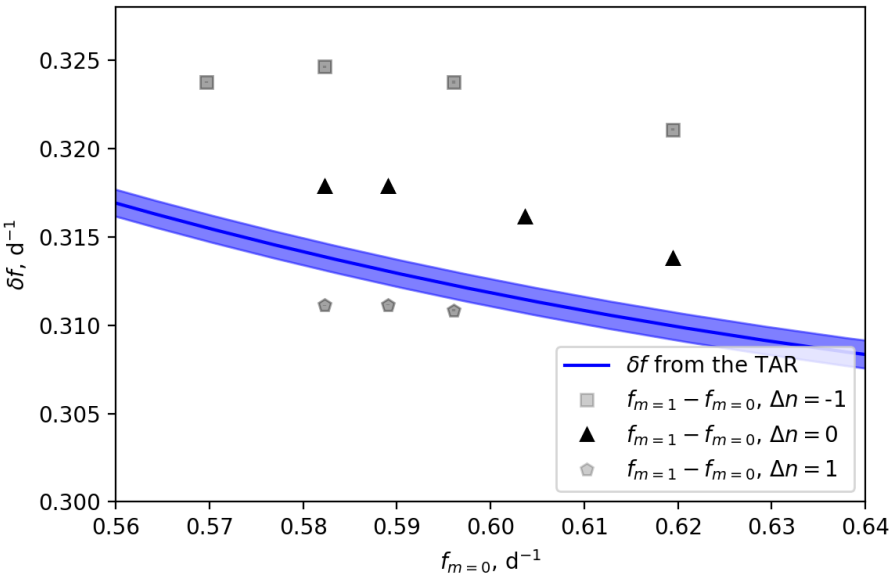

Figure 39. The observed and theoretical splittings of KIC 4952246.

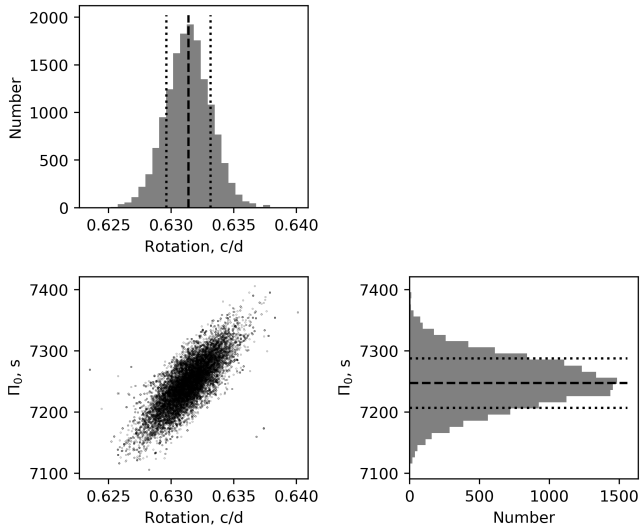

Figure 40. The 2D posterior distributions of KIC 4952246.

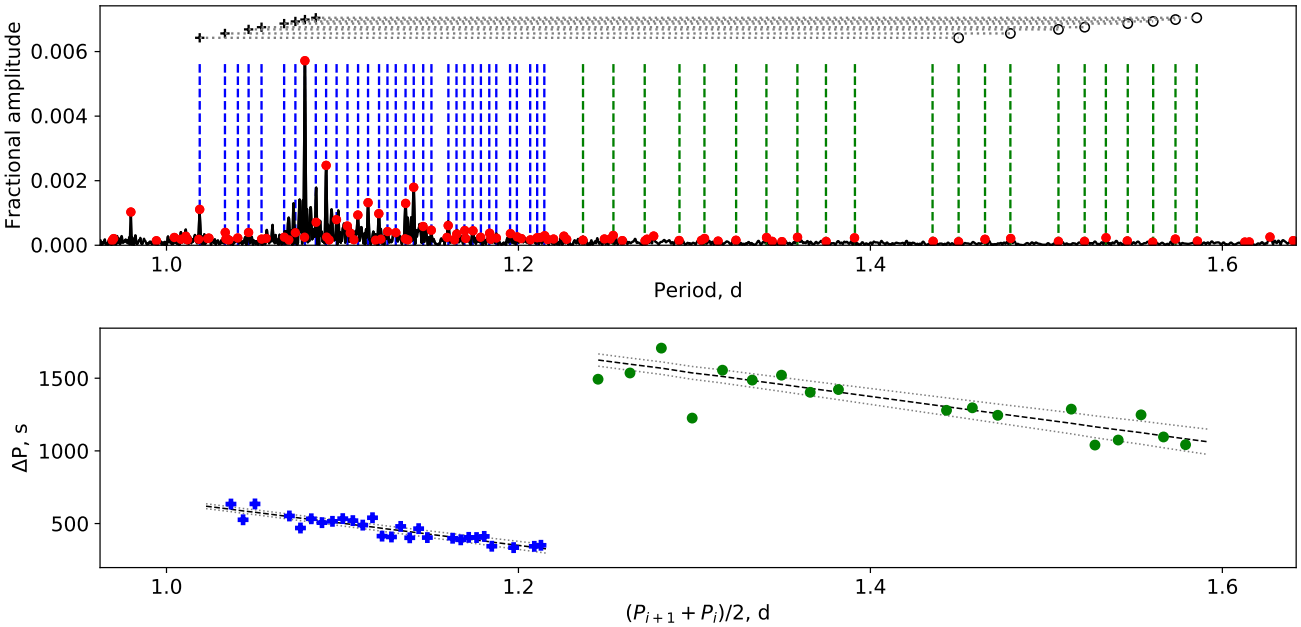

Figure 41. The period spacing patterns of KIC 12102187.

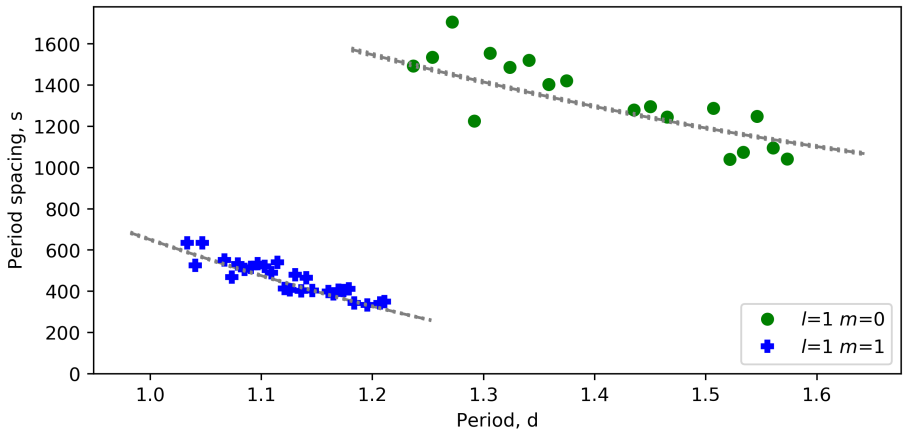

Figure 42. The best fitting period spacings of KIC 12102187.

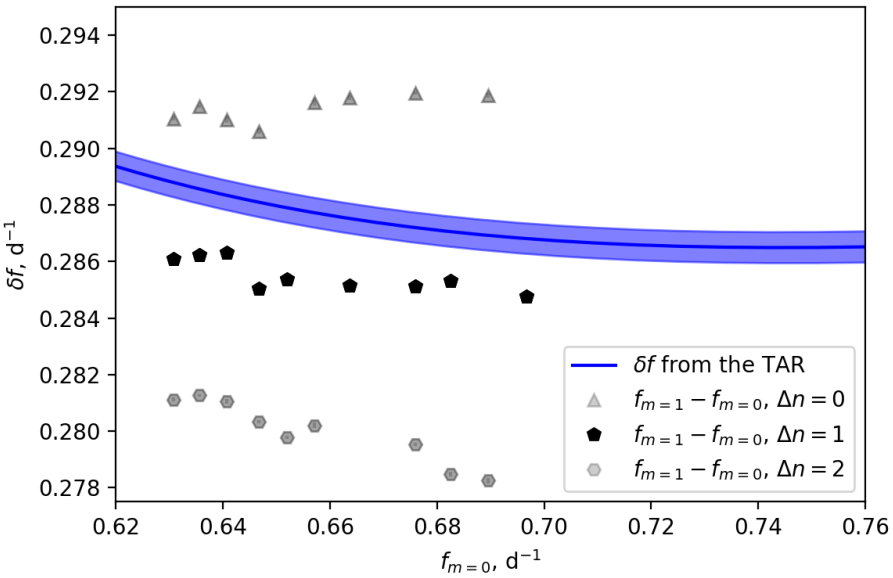

Figure 43. The observed and theoretical splittings of KIC 12102187.

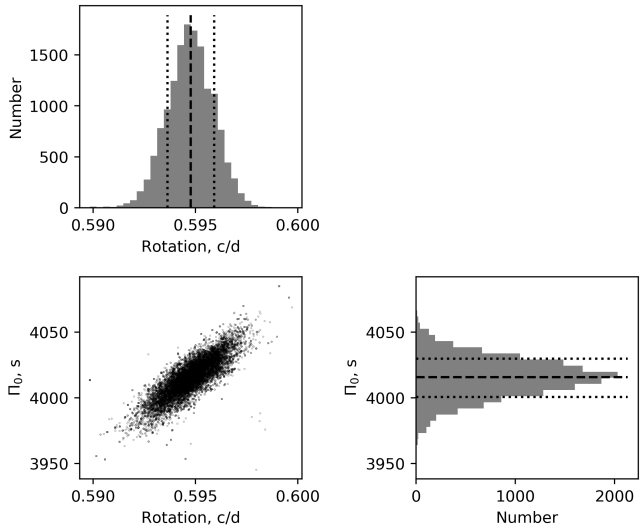

Figure 44. The 2D posterior distributions of KIC 12102187.

This paper has been typeset from a TEX/LATEX file prepared by the author.